

# Flux state and anomalous quantum Hall effect in square Kondo lattice

Xiao Chen,<sup>1</sup> Shuai Dong,<sup>1</sup> and J.-M. Liu<sup>1,2</sup>

<sup>1</sup>Laboratory of Solid State Microstructures, Nanjing University, Nanjing 210093, China

<sup>2</sup>International Center for Materials Physics, Chinese Academy of Sciences, Shenyang 110016, China  
(Dated: November 11, 2018)

The anomalous Hall effect (AHE) around the flux state in square Kondo lattice is investigated. By introducing the lattice distortion and local chirality, the square Kondo lattice can break the parity symmetry and time reversal symmetry spontaneously, and thus generate a topological nontriviality in the band structure associated with the AHE. Moreover, a possible realization of this AHE in multiferroic TbMnO<sub>3</sub> is discussed.

PACS numbers: 75.10.Jm, 75.30.Mb, 75.47.Lx

In condensed matters, novel spin orders often lead to novel physical phenomena. For instance, some multiferroics have a spiral spin order which breaks the spatial inversion symmetry and gives rise to ferroelectric polarization, which's origin is completely different from conventional ferroelectricity [1, 2]. This spiral spin order can be scaled by a vector spin chirality (VSC)  $\mathbf{S}_i \times \mathbf{S}_j$  and has become an important concept in the physics of spin current and spin liquid [3, 4]. Besides the VSC, there is another scalar spin chirality defined by:

$$\chi_{ijk} = \mathbf{S}_i \cdot (\mathbf{S}_j \times \mathbf{S}_k), \quad (1)$$

which breaks the parity (P) and time reversal (T) symmetry and was first proposed by Wen *et al* [5]. It is clear that chirality  $\chi$  would be nonzero for a noncoplanar spin order.

On the other hand, recent studies showed that the noncoplanar spin order is relevant to the intrinsic anomalous Hall effect (AHE) observed in Kondo lattice system, in which the noncoplanar background spin texture acts as a gauge field for itinerant electrons propagating in the lattice [6, 7, 8, 9, 10, 11, 12, 13, 14, 15]. Generally speaking, the intrinsic AHE has the topological origin and can be characterized by the Berry phase and Chern number. To manifest this mechanism, the system should break the P-symmetry and T-symmetry spontaneously and simultaneously [15, 16]. For a Kondo lattice model, the T-symmetry can be violated for those spin configurations with the local spin chirality, while the P-symmetry can be broken in some geometrically frustrated lattices. For instance, Ohgushi *et al* once discussed the AHE on Kagome lattice where a finite local spin chirality in the three-site unit cell can generate nonzero Hall conductance [6]. This model has been extended to other geometrically frustrated systems such as the three-dimensional (3D) pyrochlore lattice [7, 8, 9]. Therefore, a geometrically frustrated lattice with spin chirality would be of significance in terms of AHE physics.

Unfortunately, the square lattice usually has no geometrically frustrated structure, and thus it is not easy to violate the P-symmetry since the chiralities on adjacent plaquettes tend to cancel each other due to the

lattice symmetry and thus the AHE becomes hard to realize in the square lattice. However, the square lattice (and its distorted forms) takes up the majority in the practical Kondo lattice materials such as colossal magnetoresistance manganites [17] and Fe-based pnictide superconductors [18]. Besides, the realization of AHE on the square lattice is also fundamentally important and physically interesting [19, 20].

In this paper, the AHE on the Kondo square lattice is realized theoretically by introducing two mechanisms to break the P-symmetry. One is to induce some lattice distortions which can lead to the change of hopping amplitude of itinerant electrons. The other is to construct a special unit cell which breaks the P-symmetry. These two mechanisms are different from the previous considered spin-orbit interaction (SOI) which can directly generate topological nontriviality in the band structure and associate with the AHE [15, 16, 21]. Our discussion will be primarily restricted to a 'flux' state at the half filling of one-band Kondo model. We hope that these two mechanisms can be alternating approaches (other than the SOI mechanism) to the AHE in the square lattice, and eventually realized in some real materials.

The Hamiltonian of one-band Kondo lattice model on the two-dimensional (2D) square lattice can be written as: [17]

$$\begin{aligned} H = & - \sum_{NN} t_1 c_{i,\sigma}^\dagger c_{j,\sigma} - \sum_{NNN} t_2 c_{i,\sigma}^\dagger c_{k,\sigma} \\ & - J_H \sum_i \mathbf{S}_i \cdot c_{i,\alpha}^\dagger \sigma_{\alpha\beta} c_{i,\beta} \\ & + J_1 \sum_{NN} \mathbf{S}_i \cdot \mathbf{S}_j + J_2 \sum_{NNN} \mathbf{S}_i \cdot \mathbf{S}_j, \end{aligned} \quad (2)$$

where the first term describes the electron hopping between the nearest-neighbor (NN) sites, and the hopping amplitude  $t_1$  is taken as the energy unit. The second term is the electron hopping between the next-nearest-neighbor (NNN) sites. In the following,  $t_2$  is arbitrarily set as 0.25 as an example, since the AHE result is qualitatively independent of its exact value as long as it is nonzero, which will be further discussed below. The third

term is the Hund coupling linking the itinerant electrons with the background spins  $\mathbf{S}$  (assumed classical and normalized as  $|\mathbf{S}| = 1$ ) where  $J_H$  is the coupling factor. The last two terms are the antiferromagnetic (AFM) superexchanges between the background spins with  $J_1$  and  $J_2$  as the coefficients for the NN and NNN sites respectively. This model has been extensively investigated for various transitional metals' oxides, and more details of this model can be found in Ref. 17.

For the third term, by applying a canonical transformation, the Hamiltonian can be simplified by adopting the site-dependent spin-polarization axis. In the  $J_H \rightarrow \infty$  limit, the spin of the hopping electron is forced to align parallel to the on-site  $\mathbf{S}$ , and thus the hopping terms in the Hamiltonian can be transferred into the form  $t_{ij}^{eff} c_i^\dagger c_j$ , with the effective hopping integral:

$$\begin{aligned} t_{ij}^{eff} &= t \left[ \cos \frac{\theta_i}{2} \cos \frac{\theta_j}{2} + \sin \frac{\theta_i}{2} \sin \frac{\theta_j}{2} e^{-i(\varphi_i - \varphi_j)} \right] \\ &= t e^{i\varphi_{ij}} \cos \frac{\theta_{ij}}{2}, \end{aligned} \quad (3)$$

where  $t$  can be  $t_1$  or  $t_2$ .  $\theta$  and  $\varphi$  are the polar coordinates of spin  $\mathbf{S}$ . The phase factor  $\varphi_{ij}$  can be viewed as the gauge vector potential and  $\theta_{ij}$  is the angle between  $\mathbf{S}_i$  and  $\mathbf{S}_j$  [6]. When the itinerant electrons move along a closed loop, they can feel the induced gauge flux which is indistinguishable from the magnetic flux. This gauge flux is related to the spin chirality and leads to the AHE [6, 9, 14, 15].

For this model, the ground state can be calculated with the variational method, namely, by comparing the ground state energies of several preset spin configurations. Around half filling, when the  $J_1=J_2 > 0.15$ , the ground state is the flux state. This state has four sites in the unit cell, as shown in Fig. 1(a). In one plaquette, the neighboring background spins are perpendicular to each other. When an itinerant electron travels around the plaquette, it can acquire an additional  $\pi$  flux. In fact, this flux state was reported earlier in some similar systems [22, 23]. The flux phase can have many degenerate states by shifting and rotating the spin structures. Thus, a specific state, with  $(\mathbf{S}_1, \mathbf{S}_3)$  along the  $z$ -axis and  $(\mathbf{S}_2, \mathbf{S}_4)$  along the  $x$ -axis, will be adopted in the following study, which forms a spin order in the  $x$ - $z$  plane. In practical calculation, to remove the degeneration and stabilize this state, a small anisotropic energy  $H_2 = \sum K_\alpha S_\alpha^z$  (subscript  $\alpha=1-4$ ,  $K_1=K_3=-0.02$ ,  $K_2=K_4=0.02$ ) is also considered, which favors  $(\mathbf{S}_1, \mathbf{S}_3)$  along the  $z$ -axis and  $(\mathbf{S}_2, \mathbf{S}_4)$  in the  $x$ - $y$  plane. In fact, the flux state is with coplanar spin order and the AHE conductance is forbidden. Therefore, additional contributions should be included for allowing the AHE.

In real materials, due to the ionic size mismatch or competing exchange interactions, the square lattice would be distorted more or less. For instance, in multi-ferroic  $\text{RMnO}_3$ , the Mn-O-Mn chain is distorted in non-

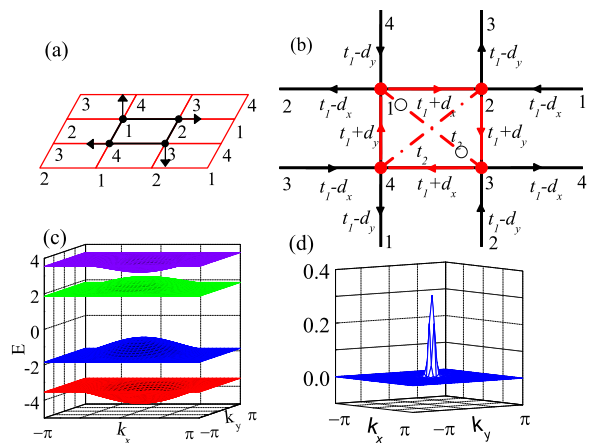


FIG. 1: (Color online) (a) The flux state with the four-site unit cell. (b) The lattice is distorted with atoms 1 and 3 moving in reversed direction with the new positions shown as open circles. The NN hopping amplitude  $t_1$  is varied correspondingly. The arrows on bonds indicate the signs of the phases of the  $t_{ij}^{eff}$ . (c) The band structure of Eq. (5) with the parameters sets  $t_{r1} = 1$ ,  $t_{r2} = 0.25$ ,  $d = 1$  and  $\phi = \pi/6$ . (d) Gauge flux density of the 3-th band of (c).

centrosymmetric manners caused by the Dzyaloshinsky-Moriya (DM) interaction, giving rise to the staggered Mn-O-Mn angles [1, 25]. For simplicity, a simple lattice distortion mode is adopted, as shown in Fig. 1(b), where the first and third cations are displaced from the original positions along the opposite directions. Due to the  $x$ - $y$  symmetry, the cation displacement along  $x$  and  $y$  are assumed to be the same. In a first order approximation, the corresponding hopping amplitude varies linearly with the tiny lattice distortion, and thus the NN hopping amplitude  $t'_1 = t_1 \pm d$  where  $d$  is the tiny amendment caused by the distortion. The influence to the NNN hopping amplitude  $t_2$  is not considered because the exact value of NNN hopping is not qualitatively important to obtain the AHE. Take one chain of the lattice for example, the hopping amplitude becomes staggeringly ordered and the P-symmetry of the lattice is broken.

With this P-symmetry broken configuration, the spin order may be not exactly confined on the  $x$ - $z$  plane, i.e., spins  $\mathbf{S}_1$  and  $\mathbf{S}_3$  tilt slightly from the  $z$ -axis and are not parallel to each other. Therefore, the local spin order may become non-coplanar, with each plaquette having a gauge flux penetrating it. In this condition, the NN hopping can be approximately modified to the following form [6]:

$$t_{ij}^{eff} = t_{r1} e^{i\varphi_{ij}} \quad (4)$$

where  $t_{r1}$  is the renormalized NN hopping amplitude. We take  $\varphi_{ij} = \phi(-\phi)$  for the hopping direction along (opposite to) the arrow direction as shown in Fig. 2(b). In addition, the renormalized NNN hopping amplitude is set as a real constant  $t_{r2}$  for simplicity. The Hamiltonian matrix for this model can be written in the momentum

space:

$$H(k) = \begin{pmatrix} 0 & e^{i\phi} f_1 & f_3 & e^{-i\phi} f_2 \\ e^{-i\phi} f_1^* & 0 & e^{i\phi} f_2 & f_3 \\ f_3 & e^{-i\phi} f_2^* & 0 & e^{i\phi} f_1^* \\ e^{i\phi} f_2^* & f_3 & e^{-i\phi} f_1 & 0 \end{pmatrix} \quad (5)$$

where  $f_1(k) = t_{r1} \cos(k_x/2) + id \sin(k_x/2)$ ,  $f_2(k) = t_{r1} \cos(k_y/2) + id \sin(k_y/2)$ ,  $f_3(k) = t_{r2} [\cos((k_x - k_y)/2) + \cos((k_x + k_y)/2)]$ . Now, the AHE conductance can be calculated. The contribution to the AHE conductance from each band is written as [6, 16]:

$$\begin{aligned} \sigma_{xy}^n &= \frac{e^2}{h} \frac{1}{2\pi i} \int_{BZ} d^2 \mathbf{k} \mathbf{z} \cdot \nabla_{\mathbf{k}} \times \mathbf{A}_n(\mathbf{k}) \\ &= \frac{e^2}{h} \frac{1}{2\pi i} \int_{BZ} d^2 \mathbf{k} \mathbf{z} \cdot \mathbf{B}_n(\mathbf{k}) \\ &= \frac{e^2}{h} C_n, \end{aligned} \quad (6)$$

where  $\mathbf{A}_n(\mathbf{k}) = \langle nk | \nabla | nk \rangle$  is the vector potential defined with the  $n$ -th wave function,  $\mathbf{B}_n(\mathbf{k})$  is the gauge flux density and  $C$  is the so-called first Chern number. At  $d = 0$  case, namely, the ideal square lattice without any distortion, the P-symmetry is maintained, leading to zero Chern number for each band. At  $d \neq 0$  case, the P-symmetry is broken. The calculation indicates that the Chern number for each band is  $C = [0, 0, 1, -1]$  at  $\phi < \pi/4$ , and  $C = [1, -1, 0, 0]$  at  $\phi > \pi/4$  (at  $\phi = \pi/4$ , the T-symmetry is conserved, corresponding to the flux state). For instance, at  $\phi = \pi/6$ , the band structure is shown in Fig. 1(c), and the gauge flux density  $\mathbf{B}(\mathbf{k})$  of the 3-th band is shown in Fig. 1(d).

For Hamiltonian Eq. (2), the nonzero NNN hopping term is essentially important to generate the topological nontriviality in the band structure. This can be intuitively understood as follows. For Eq. (5), in the large  $d$ -limit,  $f_1(k) \approx id \sin(k_x/2)$ , under the unitary transformation  $UHU^T \rightarrow H'$  [24], the Hamiltonian matrix Eq. (5) can be further decoupled into the form:

$$H' = \begin{pmatrix} h_1(k) & 0 \\ 0 & h_2(k) \end{pmatrix} \quad (7)$$

where  $h_1(k)$  and  $h_2(k)$  are both  $2 \times 2$  matrixes.

For the matrix  $h_1(k)$ , we have:

$$h_1(k) = \begin{pmatrix} d \sin \phi f_4 & -id \cos \phi f_5 - f_3 \\ id \cos \phi f_5 - f_3 & -d \sin \phi f_4 \end{pmatrix} \quad (8)$$

where  $f_4(k) = \sin(k_x/2) + \sin(k_y/2)$ ,  $f_5(k) = \sin(k_x/2) - \sin(k_y/2)$ . Around  $k = (\pi, \pi)$ , the electron can be considered as a generalized Dirac fermion and the effective Hamiltonian  $h_1(k)$  ( $h_2(k)$ ) can be treated in a similar way) is

$$h_1(k) = -\frac{t_{r2}}{2} k_x' k_y' \sigma^x + \frac{d \cos \theta}{8} (k_y'^2 - k_x'^2) \sigma^y + 2d \sin \phi \sigma^z, \quad (9)$$

where  $k_x' \equiv k_x - \pi$ ,  $k_y' \equiv k_y - \pi$ . The general form of Eq. (10) was thoroughly addressed in Ref. 16, and the corresponding Chern number for the upper and lower bands is  $C = \pm 2 \text{sgn}(t_{r2}/d)$  (at  $\phi = \pi/6$ ) where  $\text{sgn}$  is the sign operator. If  $t_{r2} = 0$ ,  $C = 0$  for both bands, indicating that the NNN hopping term is indispensable in generating the Hall conductance.

Consequently, one can argue that the lattice distortion provides an effective method to break the P-symmetry, and yet the non-coplanar spin order as the ground state is absolutely necessary. In fact, the non-coplanar spin order can also be accomplished by further taking into account the frustrated magnetic interaction. For instance, by adding the third neighbor (3rd N) superexchange interaction  $H_3 = \sum_{3rdN} J_3 \mathbf{S}_i \cdot \mathbf{S}_j$  to the distorted Kondo lattice model described by Eq. (2), the original flux state at the half filling evolves into a state in Fig. 2(a). In this condition, the unit cell expands to eight-site and is formed with two interlaced square sublattices, compared with the original four-site unit cell (formed by  $\mathbf{S}_6$ ,  $\mathbf{S}_3$ ,  $\mathbf{S}_7$  and  $\mathbf{S}_4$ ). For this spin configuration, we can straightly calculate the Hall conductivity at zero temperature by using the Kubo formula [16]:

$$\sigma_{xy} = \frac{e^2}{h} \frac{1}{2\pi i} \sum_{nmk} \frac{\langle nk | J_x | mk \rangle \langle mk | J_y | nk \rangle - h.c.}{[\varepsilon_n(k) - \varepsilon_m(k)]^2}, \quad (10)$$

where  $|nk\rangle$  is the occupied state and  $|mk\rangle$  is the empty state.  $\varepsilon$  denotes the eigen-energy.  $J_x$  ( $J_y$ ) is the  $x$  ( $y$ ) components of the current operator. The calculation is performed in momentum space, with the summation over all the eight bands. For example, with a finite  $J_3$  (see Fig. 2(a)'s caption),  $\sigma_{xy} = 0.13 e^2/h$  at half filling, clearly indicating that this ground state does exhibit the AHE. Besides, the Hall conductance as the function of conduction electron density  $n$  is shown in Fig. 2(b), with the spin configuration fixed as Fig. 2(a). The curve in Fig. 2(b) fluctuates dramatically, showing that the AHE is sensitive to  $n$  [21].

Interestingly, additional investigation of the ground state in Fig. 2(a) indicates that besides the lattice distortion, this special unit cell structure also breaks the P-symmetry spontaneously. Thus for this unit cell structure, with the local spin chirality, the band structure can lead to nonzero Chern number and Hall conductance even without any lattice distortion or NNN hopping. For the local spin order shown in Fig. 2(c), the eight bands are topologically nontrivial and the corresponding Chern number  $C = [1, -1, 0, 0, 0, 0, -1, 1]$ , with the gauge flux density of the 1-th band shown in Fig. 2(d). In fact, due to the frustrated magnetic interaction, the unit cell could involve more sites and become even larger with the parity violation satisfied. For instance, for Eq. (2), with large  $J_1$  ( $J_2 = J_1$ ) and low  $n$ , the variational calculation indicates the ground state is with the coplanar spiral order. This coplanar spiral order can evolve into the 3-D spi-

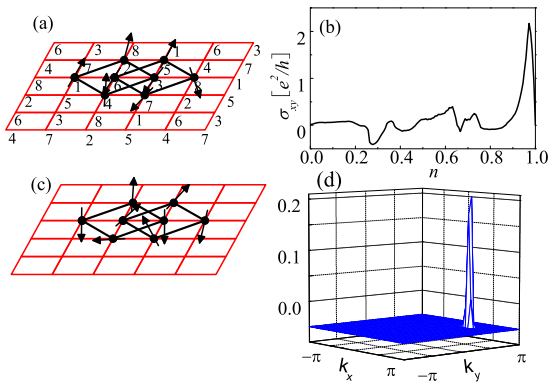


FIG. 2: (Color online) (a) The ground state with the parameter sets  $J_1 = J_2 = 0.04$ ,  $J_3 = 0.025$ ,  $t_1 = 1$ ,  $t_2 = 0.25$ ,  $d = 0.4$  and  $n = 0.5$ . The unit cell expands to eight-site here. (b) The Hall conductance as a function of the conduction electron density  $n$  with the spin order shown in (a). (c) An example of the nontrivial spin order in the special eight-site unit cell. (d) Gauge flux density  $\mathbf{B}(k)$  of the 1-th band with the spin order shown (c).

ral order by including the  $H_2$  and  $H_3$  term. However, in this case, the unit cell also expands dramatically, and the band calculation becomes much more challenging. The ground state we address here seems to be a special case with a relatively small unit cell.

Although the calculation of Eq. (2) and the addressed two mechanisms are more or less theoretically oriented, their realization in real systems is still possible. For example, multiferroic  $\text{TbMnO}_3$  is a promising candidate to illustrate these two mechanisms and observe the AHE. In  $\text{TbMnO}_3$ , besides the  $\text{GeFeO}_3$ -type distortion, which forms the Mn-O-Mn zigzag chain, the DM interaction is also present [25]. In this case, due to the spiral order of the background spin, the Mn-O-Mn zigzag chain is distorted with all the oxygen ions displaced in the same direction [25]. Therefore the adjacent Mn-O-Mn angles are different, leading to the staggered order of the effective Mn-Mn hopping amplitude and broken parity symmetry. For  $\text{TbMnO}_3$ , neutron scattering experiments confirmed that the background  $t_{2g}$  electrons form a coplanar spiral order. To excite the noncoplanar spin order, a magnetic field with its direction different from the spin order plane can be applied, allowing the nonzero Hall conductance. In addition, the ferroelectric polarization in  $\text{TbMnO}_3$  aligns along the direction of  $\mathbf{e}_{ij} \times (\mathbf{S}_i \times \mathbf{S}_j)$ . Therefore, the noncollinear ferroelectric polarization should be expected for this non-coplanar spin order. Moreover, the  $\text{Tb}^{3+}$  cations can be doped by other +4 cations, which can modulate the itinerant electrons density and directly control the AHE [21]. However, for these calculations, a more practical two-orbital model should be employed.

In conclusion, we have studied the Kondo lattice model on a square lattice with frustrated super-exchange interactions. The calculated nonzero Hall conductance is attributed to two distinct mechanisms, one is the lattice

distortion and the other is the locally nontrivial spin order. Both of these mechanisms break the P-symmetry and can generate the AHE spontaneously.

The authors acknowledge with E. Dagotto, Q. H. Wang, N. Nagaosa and R. Shindou for fruitful discussions.

- 
- [1] T. Kimura, Annu. Rev. Mater. Res. **37**, 387 (2007).
  - [2] K. F. Wang, J.-M. Liu, and Z. F. Ren, Adv. Phys. **58**, 321 (2009).
  - [3] H. Katsura, N. Nagaosa, and A. V. Balatsky, Phys. Rev. Lett. **95**, 057205 (2005).
  - [4] J. H. Park, S. Onoda, N. Nagaosa, and J. H. Han, Phys. Rev. Lett. **101**, 167202 (2008).
  - [5] X. G. Wen, F. Wilczek, and A. Zee, Phys. Rev. B **39**, 11413 (1989).
  - [6] K. Ohgushi, S. Murakami, and N. Nagaosa, Phys. Rev. B **62**, R6065 (2000).
  - [7] R. Shindou, and N. Nagaosa, Phys. Rev. Lett. **87**, 116801 (2001).
  - [8] I. Martin, and C. D. Batista, Phys. Rev. Lett. **101**, 156402 (2008).
  - [9] Y. Taguchi, Y. Oohara, H. Yoshizawa, N. Nagaosa, and Y. Tokura, Science **291**, 2573 (2001).
  - [10] A. Neubauer, C. Pfleiderer, B. Binz, A. Rosch, R. Ritz, P. G. Niklowitz, and P. Boni, Phys. Rev. Lett. **102**, 186602 (2009).
  - [11] M. Lee, W. Kang, Y. Onose, Y. Tokura, and N. P. Ong, Phys. Rev. Lett. **102**, 186601 (2009).
  - [12] S. D. Yi, S. Onoda, N. Nagaosa, and J. H. Han, arXiv:0903.3272.
  - [13] K. Taguchi, and G. Tatara, arXiv:0811.0890.
  - [14] S. Onoda, and N. Nagaosa, Phys. Rev. Lett. **90**, 196602 (2003).
  - [15] N. Nagaosa, J. Sinova, S. Onoda, A. H. MacDonald, and N. P. Ong, arXiv:0904.4154.
  - [16] M. Onoda, and N. Nagaosa, J. Phys. Soc. Jpn. **71**, 19 (2002).
  - [17] E. Dagotto, T. Hotta, and A. Moreo, Phys. Rep. **344**, 1 (2001).
  - [18] Y. Kamihara, T. Watanabe, M. Hirano, and H. Hosono, J. Am. Chem. Soc. **130**, 3296 (2008).
  - [19] N. Goldman, A. Kubasiak, P. Gaspard, and M. Lewenstein, Phys. Rev. A **79**, 023624 (2009).
  - [20] N. Goldman, A. Kubasiak, A. Bermudez, P. Gaspard, M. Lewenstein, and M. A. Martin-Delgado, Phys. Rev. Lett. **103**, 035301 (2009).
  - [21] K. S. Takahashi, M. Onoda, M. Kawasaki, N. Nagaosa, and Y. Tokura, Phys. Rev. Lett. **103**, 057204 (2009).
  - [22] M. Yamanaka, W. Koshibae and S. Maekawa, Phys. Rev. Lett. **81**, 5604 (1998).
  - [23] D. F. Agterberg and S. Yunoki, Phys. Rev. B **62**, 13816 (2000).
  - [24] In the large  $d$ -limit, we take  $f_1(k) \approx id \sin(k_x/2)$ . This approximation is not accurate especially at  $k_x = 0$ . We take this approximation here just to emphasize the importance of  $t_{r2}$ .
  - [25] T. Arima, A. Tokunaga, T. Goto, H. Kimura, Y. Noda, and Y. Tokura, Phys. Rev. Lett. **96**, 097202 (2006).